Dynamics of laser generation in single-mode microstripe semiconductor laser bar (1065 nm) operating in gain-swithching mode

© A.A. Podoskin, I.V. Shushkanov, A.E. Rizaev, V.A. Krychkov, A.E. Grishin, N.A. Pikhtin

Ioffe Institute,
194021 St. Petersburg, Russia
E-mail: podoskin@mail.ioffe.ru

Received November 17, 2023
Revised January 11, 2024
Accepted January 31, 2024

The study investigates microstripe bars of optically isolated single-mode lasers based on heterostructures with double asymmetry, operating under sub-nanosecond current pulse pumping conditions. For microstripe bars with different filling densities of the emitting aperture, the effect of time delay dispersion of various stripes' turn-on is demonstrated, with a maximum difference up to 50 ps. The developed microstripe bar designs demonstrate stable zero mode lasing. The microstripe bar consisting of 10 stripes with a 6 *mu*m width and a stripe period of 20 μm demonstrates pulses with a peak power of 3 W and a duration of 140 ps under 0.4 ns current pulses pumping.

Keywords: semiconductor laser, laser bar, gain switching.

DOI: 10.61011/0000000000

1. Introduction

The issue of design of compact, efficient, and affordable sources of high-power sub-nanosecond laser radiation based on semiconductor lasers is a currently relevant one. Its practical importance rests on the strong application potential of such sources, which may be used in lidars (light detection and ranging) for autonomous vehicles, free-space communication lines, and as reference sources for solid-state amplifiers. Available solutions relying on fiber and solid-state lasers have the capacity to generate pulses of a required duration and power, but the potential for enhancement of their size and weight characteristics is limited. In addition to the mentioned characteristics, certain other parameters, such as the repetition rate in compact rangers for autonomous vehicles that should be raised to the MHz level, require improvement. Radio photonics applications requiring multichannel transmission of high-frequency and high-power electromagnetic radiation are also advancing rapidly. Specifically, optical systems based on high-power pulsed nanosecond semiconductor lasers and photodetectors operated in the photovoltaic regime were demonstrated in [1]. Transmission along a fiber line with an optical carrier and generation of bipolar electric pulses at load, which ensure the generation of an ultrawideband signal with a center frequency of 750 MHz, were implemented in these optical systems [1]. Further progress in this direction may involve the development of approaches to generation of sub-nanosecond pulses that should allow one to reach GHz frequencies.

Owing to their low power, currently available solutions based on telecommunication lasers cannot support the transition to sub-nanosecond pulse durations in discussed applications [2]. The principles of generation of low-power optical data signals with the shape and the amplitude of a laser pulse dictated by the shape and the amplitude of a pump current pulse are ill-suited for generation of high-power laser pulses. This is attributable to the high complexity of the task of designing generators of pump current pulses with the needed amplitude (tens of amperes) and duration (below 1 ns). One feasible method for generation of high-power sub-nanosecond laser pulses involves the use of high-power multimode semiconductor lasers operating in the gain switching regime [3,4]. The duration of a pump current pulse may in this case exceed considerably the duration of a generated laser pulse. Several studies focused on the approaches to optimization of laser heterostructures [4–7] and cavity parameters [6] have been published in recent years. The existence of an optimum set of heterostructure and cavity parameters (cavity length and reflection coefficients) for generation of pulses of the needed power and duration was established [6]. In this context, widening of the emitting aperture may be a solution allowing one to raise the power while maintaining the optimum structure and cavity characteristics. Sub-nanosecond dynamics of radiation of high-power semiconductor lasers operating at 1060 nm for laser diodes with an emitting aperture width of 800 μm under pumping by 3-ns-long current pulses was examined in [8]. It was found that the lasing turn-on delay is inhomogeneous along the aperture and the magnitude of this inhomogeneity is as large as several hundred picoseconds. This leads to broadening of a generated pulse and reduces its peak power, which is the principal factor limiting the application of such designs for generation of short laser pulses in the gain switching regime. In addition, the use of wide apertures is associated with a multimode lasing structure, which also reduces the efficiency of coupling to an optical fiber. Various designs of a lateral waveguide [9–11] aimed at enhancing the quality of the mode structure have been proposed. Single-mode microstripe bars were

examined in [9]. The potential to generate pulses with a peak power of 25 W and a duration of 130 ns was demonstrated. Notably, the parallel far field maintained a nearly unchanged Gaussian-like structure within the entire power range. Sub-nanosecond dynamics of such structures has not been investigated yet. In the present study, the specifics of generation of high-power sub-nanosecond laser pulses in the gain switching regime with various designs of microstripe bars of semiconductor heterostructures emitting at a wavelength of 1060 nm and characterized by a high lateral field quality are examined.

2. Experimental samples and research technique

A laser heterostructure design with double asymmetry and a widened waveguide was used. Asymmetry was manifested both in the positioning of the active region and in the emitter compositions. The design was optimized toward reducing internal optical losses and obtaining a suppressed radiation pattern in the perpendicular far field.

This heterostructure (Figure 1) featured a wide-band $Al_xGa_{1-x}As$ ($x = 10\%$) waveguide 1.6 μm in thickness and an active region based on two InGaAs quantum wells ($\lambda = 1070$ nm) shifted toward the *p*-emitter. The waveguide layer was positioned between the $Al_xGa_{1-x}As$ ($x = 35\%$) *p*-emitter and the $Al_xGa_{1-x}As$ ($x = 15\%$) *n*-emitter. A heterostructure of the chosen design was grown by MOS hydride epitaxy in a vertical reactor. Two types of samples were fabricated next. Samples of the first type were prepared for standard characterization and were semiconductor lasers of a mesastripe design with a width of 100 μm. Samples of the second type (bars of ten microstripes with a width of 6 μm) were prepared for the examination of dynamic characteristics. Two variants of microstripe bars were fabricated for experiments: (1) with mesagrooves 14 μm in width and an overall bar width of 185 μm — HDMSA (High Dense Micro-Stripe Array); (2) with mesagrooves 39 μm in width and an overall bar width of 410 μm — LDMSA (Low Dense Micro-Stripe Array). As was demonstrated above, the main feature of a microstripe bar is the capacity to generate high-power laser radiation with a radiation pattern structure close to the single-mode one. This may be achieved through the use of a single-mode laser bar. The depth of mesagrooves between stripes in a bar, which specify the power of a lateral waveguide, is an important parameter in this case. Two boundary operating regimes of a microstripe bar with different powers of a lateral waveguide may be distinguished. The first regime is implemented when separating mesagrooves are shallow and a low-power lateral waveguide is used. Weak optical confinement of lateral modes of each microstripe is typical of this regime. providing an opportunity to form a common waveguide that encompasses the entire microstripe bar

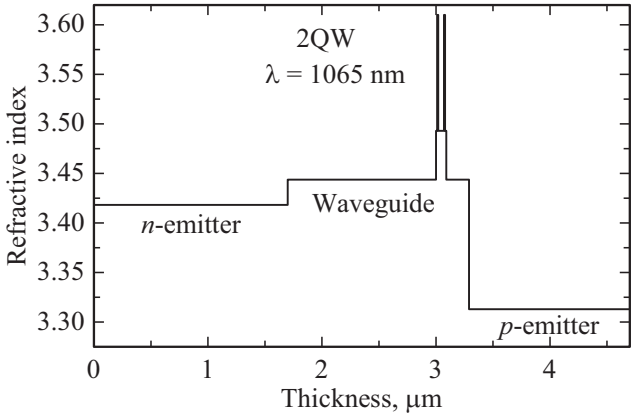

Figure 1. Laser heterostructure design.

structure. However, this regime is highly sensitive to external conditions (pump current amplitude, pulse duration, and temperature). In addition, a wide aperture makes it rather hard to fulfill single-mode lasing conditions in this structure. The second regime is implemented with the use of deep mesagrooves and a high-power lateral waveguide. The optical coupling between microstripes may be neglected in this case, and the parallel field is specified by the waveguiding characteristics of an individual mesastripe of a bar. The waveguiding properties of the two-dimensional mesastructure of an individual mesastripe were calculated for the chosen heterostructure design, which supports single-mode lasing, in order to fulfill the conditions of zero-mode generation. Experimental samples of microstripe bars were fabricated based on the results of calculations. Their cavity length was 3 mm. Antireflective (5%) and reflective (98%) coatings were deposited onto the end faces of emitters. Samples of microstripe bars were then mounted with the *p*-contact facing down onto a radio-frequency line providing matching with a source that pumped a microstripe bar with current pulses with a half-amplitude duration of ~ 0.4 ns and an amplitude up to 18.5 A. This RF line was designed so as to ensure electrical connection, transmission of a pump pulse, and correct measurements with an Agilent 54855A oscilloscope. The experimental setup based on the RF line allowed for correct measurements of the shape and power of optical radiation pulses with an optical radiation collection arrangement based on aspherical optics. The optical arrangement provided an opportunity both to collect radiation into a moderate-power meter and to introduce an optical beam into input fibers of photodetectors and optical spectrum analyzers. It was fitted with precision mechanical adjusters needed to tune the experimental setup for measurement of the optical signal of individual emitters. The optical signal shape was recorded by a New Focus 1444-50 high-speed photodetector (20 GHz) and an Agilent 86117A stroboscopic oscilloscope (50 GHz). The average radiation power was measured by an Ophir 3A-P-12-FS thermal

sensor. An Ophir BeamStar FX 66 CCD array was used to record the radiation pattern.

3. Experiment

Watt-ampere characteristics of semiconductor lasers with a stripe contact 100 μm in width and different cavity lengths were measured in order to determine the heterostructure properties. Internal optical losses and the internal quantum efficiency were calculated from these dependences: 0.3 cm^{-1} and 95%, respectively. The corresponding transparency current was 130 A/cm^2. Far-field measurements in the perpendicular direction were performed by scanning with a slit. The obtained distributions demonstrated that the far field remains stable within the entire studied range of pump currents; the FWHM divergence was 25°. Measurements of the watt-ampere characteristics of microstripe bars of both designs in the continuous regime revealed a slope of 1.01 W/A for samples with a cavity length of 3 mm (AR-HR).

The operating regimes of microstripe bars under subnanosecond pumping were examined in two stages. At the first stage, the integral dynamics of lasing was determined for HDMSA and LDMSA microstripe bars. Figure 2 presents the typical shapes of integral optical power pulses within a wide range of pump current amplitudes. The overall shape of pulses did not change with stripe period in a bar, confirming the lack of optical coupling between individual stripes. When the pump current amplitude increases, optical pulses acquire an extended tail that is substantially longer than a pump current pulse. Since the regime of generation of just the so-called „single peak“ (the first relaxation peak of a nonlinear oscillation transient lasing process under pulsed pumping [4,5,12]) is of the utmost interest, the results reported below correspond to pumping conditions allowing for single-peak operation. In the present study, a pulse was considered to be isolated if the amplitude of its extended tail was $\leq$ 5% of the maximum one.

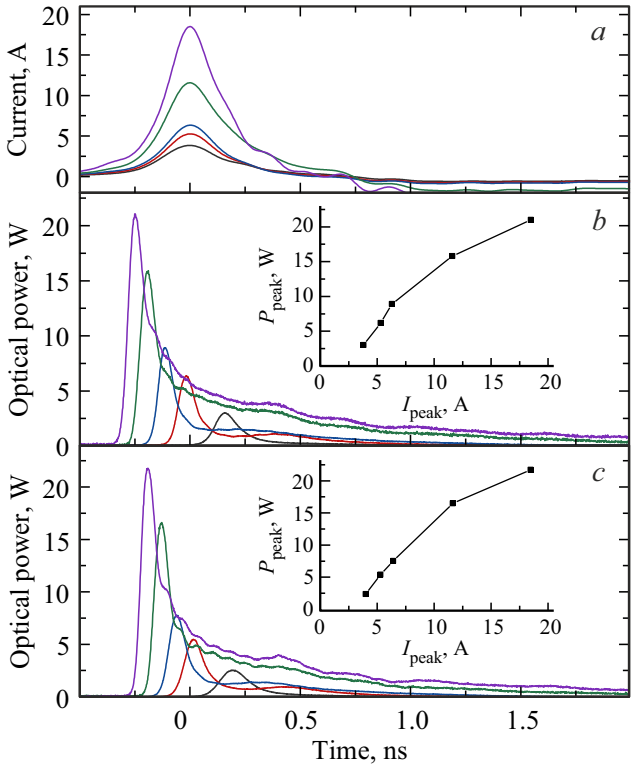

Figure 2. *a* — Shapes of pump current pulses; *b*, *c* — typical shapes of optical power pulses (not synchronized in time) at different amplitudes of pump current pulses for (AR-HR) microstripe bars with 10 stripes, a cavity length of 3 mm, and a period of 20 (*b*) and 45 μm (*c*). Dependences of the peak optical power on the pump current amplitude are shown in the insets. (A color version of the figure is provided in the online version of the paper).

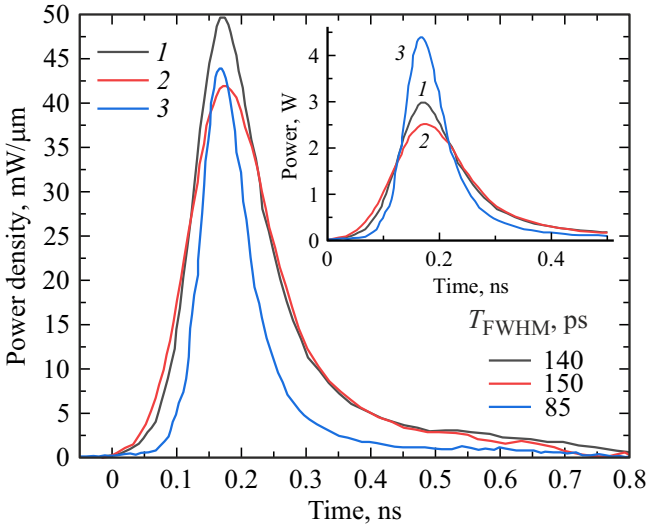

Figure 3. Power per 1 μm of the emitting aperture width and total power (inset) for samples of microstripe bars with 10 stripes and the following stripe periods: *1* — 20 μm (HDMSA); *2* — 45 μm (LDMSA). Curve *3* corresponds to an emitter with a 100-μm-wide continuous aperture.

Figure 3 shows the shapes of optical pulses in the single first pulse regime for microstripe bars with periods of 20 and 45 μm and for samples of emitters with a 100-μm-wide continuous aperture fabricated from the same heterostructure. The peak power for HDMSA and LDMSA microstripe bars was 3 and 2.5 W, respectively. The power per unit emitting aperture width was 50 and 42 mW/μm for HDMSA and LDMSA designs, respectively. These values are similar to the results for emitters with a 100-μm-wide continuous aperture and a cavity length of 1 mm–44 mW/μm. It also follows from the measurement data on lasing dynamics that: (1) the microstripe bar design (distance between individual optically uncoupled stripes) does not exert a significant influence on the maximum optical power and the shape of an optical pulse; (2) the width of an optical pulse of microstripe bars exceeds the

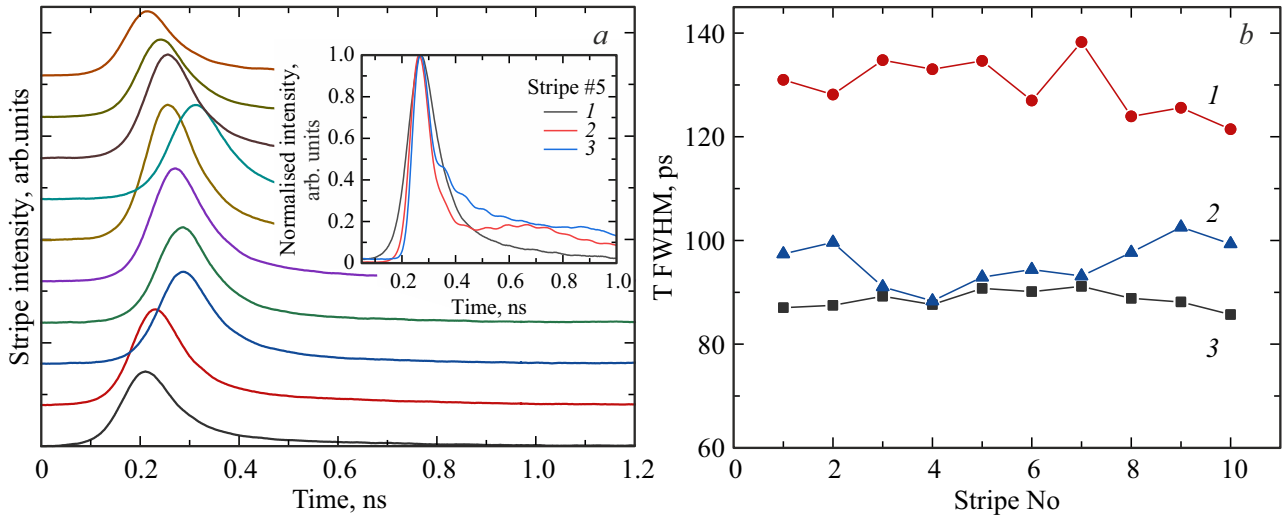

Figure 4. *a* — Intensities of emission of individual stripes in a bar with a period of 45 μm (LDMSA) at a pump current of 4.1 A; normalized intensities of emission of stripe 5 at a pump current of 4.1 (*1*), 6.5 (*2*), and 18.5 A (*3*) are shown in the inset. *b* — half-amplitude durations of pulses for various stripes of a bar under different pump currents: *1* — 4.1, *2* — 6.5, *3* — 18.5.

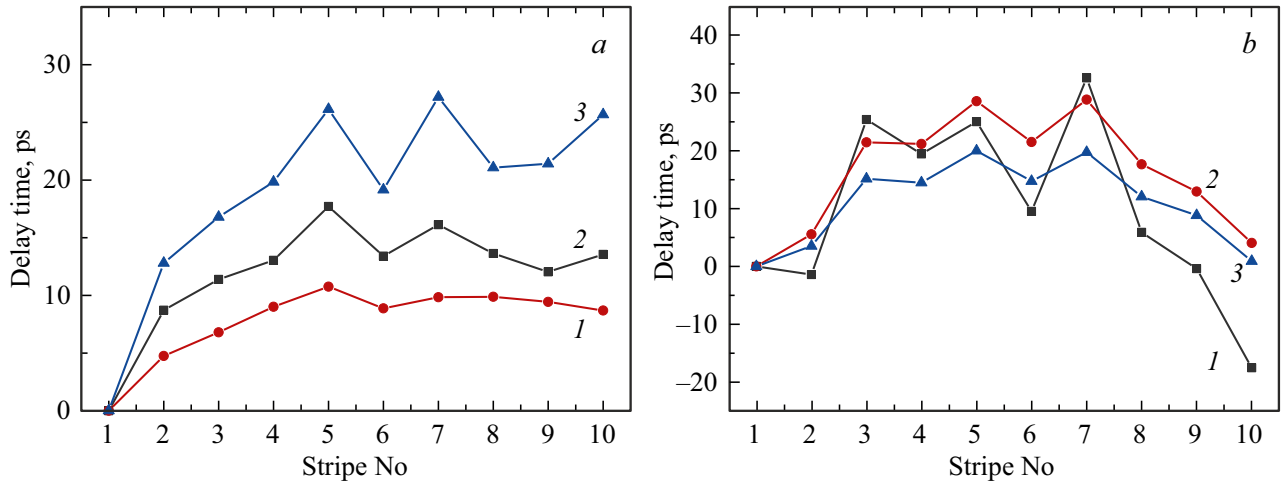

Figure 5. Distribution of relative (the first outermost stripe is taken as zero time) lasing turn-on delay times over stripes at different pump current amplitudes for microstripe bars with a period of *a* — 20 μm (HDMSA) and *b* — 45 μm (LDMSA). The pump current amplitudes are as follows: *1* — 4.1, *2* — 11.7, and *3* — 18.5 A.

width of a pulse of an emitter with a continuous aperture. Specifically, the FWHM width of an optical pulse was as large as 140–150 ps and 85 ps for microstripe bar samples and samples with a 100-μm-wide continuous aperture, respectively.

Pulses from individual stripes were measured in order to clarify the reason behind broadening of an integral optical pulse of a microstripe bar (Figure 4). It can be seen that the pulse duration in the single-peak regime is as high as 130 ps at a low pump current amplitude and decreases to 90 ps as the pump current rises, inducing additionally the emergence of oscillations and the formation of an extended pulse tail. Figure 5 presents the distributions of relative lasing turn-on delay times for different stripes of a microstripe bar.

The obtained distributions demonstrate that the outermost stripes (*1* and *10* in Figure 5) in a bar turn on earlier than the central ones (*5* and *6* in Figure 5). The observed effect is typical of pumping of both multimode emitters with a single continuous aperture and arrays of multimode emitters [8] by pulses with sub-nanosecond current fronts. Specifically, the spread of delay times of emergence of the first optical peak was 350–450 ps for an emitter with a 800-μm-wide continuous aperture [8] operated with the same pulsed current pumping circuit. The observed spread for microstripe bars is significantly smaller (even with their overall width taken into account): 20–25 ps at a microstripe bar width of 185 μm for HDMSA (Figure 5, *a*) and up to 50 ps at a bar width of 410 μm for LDMSA (Figure 5, *b*).

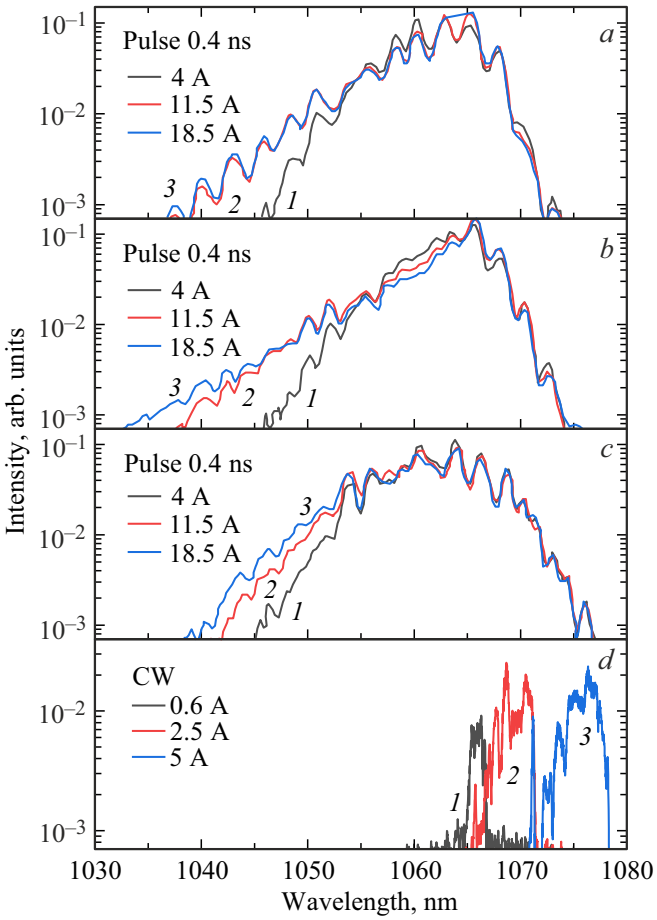

Figure 6. Lasing spectra for samples with a cavity length of 3 mm (AR-HR): *a* — microstripe bars with a period of 20 μm (HDMSA), *b* — microstripe bars with a period of 45 μm (LDMSA), and *c* — a sample with a 100-μm-wide continuous aperture pumped by pulses with a duration of 0.4 ns and an amplitude of 4 (*1*), 11.5 (*2*), and 18.5 A (*3*); *d* — a sample with a 100-μm-wide continuous aperture pumped by continuous current with an amplitude of 0.6 (*1*), 2.5 (*2*), and 5 A (*3*).

It is evident that the spread of delay times is proportional to the overall width of a microstripe bar. Experimental data (Figure 5) also reveal that the spread of delay times grows narrower as the pump current increases. The spread decreases from 25 to 10 ps for HDMSA samples and from 55 to 20 ps for LDMSA ones. Thus, in the single first optical pulse regime, the turn-on delay spread together with the widths of pulses from individual stripes provide an explanation for the duration of an integral pulse of a microstripe bar (140–150 ps; see Figure 3). The observed difference in duration between pulses of individual stripes and samples with a 100-μm-wide continuous aperture may be attributed to the following effects: (1) additional losses introduced by bounding mesagrooves are present for single-mode stripes; (2) the modal differential gain of a microstripe bar is lower than that of a continuous stripe, since the lasing mode of a narrow stripe has a nonuniform overlap with the pumped active region [12]. However, the first effect is insignificant in the proposed design, since microstripe bars have high emissive efficiencies (the slope of watt-ampere characteristics decreases only slightly compared to the one of 100-μm stripe emitters). As for the second effect, a weaker uniformity of overlap between the pump region and the optical generation region is confirmed by the results of simulation of the transverse profile of a lasing mode. Specifically, the calculated FWHM value of the profile is 4.1 μm, which is substantially smaller than the width of a mesastripe (6 μm). At the edges of a mesastripe, the calculated lasing mode intensity was 14% of the maximum one.

Lasing spectra were also measured for HDMSA and LDMSA microstripe bars under different pumping conditions. It follows from the obtained spectra (Figure 6) and the data presented in [9] that, if compared with continuous pumping, the lasing spectrum in the nonstationary lasing regime (gain switching regime) under pumping by sub-nanosecond current pulses expands toward shorter wavelengths. A similar behavior was noted in the studies of emitters with a bulk active region [4]. It is known that the concentration of carriers in the active region in nonstationary lasing regimes exceeds at certain instants the values typical of stationary lasing at the same pump current [12]. This leads to the inclusion of new spectral lines into lasing, and the integral spectrum becomes broader as a result, while its maximum, in complete agreement with the obtained experimental data, shifts toward shorter wavelengths.

The radiation pattern of HDMSA and LDMSA microstripe bars was examined with the use of a calibrated CCD array. In contrast to the emitters with a wide continuous aperture [8], the studied samples had a stable pattern in the far field, which corresponded to single-mode lasing of individual stripes of these bars (Figure 7). The experimental divergence in the single peak regime in the plane of heterostructure layers was 7.7–8 and 6.9–7.1° for HDMSA and LDMSA designs, respectively (Figure 7, *c*). In the perpendicular plane, the divergence for HDMSA and LDMSA microstripe bars was 22.8 and 24.9°, which agrees also with calculated data.

4. Conclusion

The obtained data revealed certain features of emissive characteristics of microstripe bars operating in the gain switching regime. First and foremost, it was demonstrated that an individual laser pulse from a microstripe bar gets broadened to 140–150 ps, while lasers with a 100-μm-wide continuous aperture produce pulses with a duration of 85 ps. This is attributable both to broadening of pulses from individual stripes and to the variation of lasing turn-on delay times from one stripe to the other. This has a negative effect on the peak power. Notably, the density of stripes in a bar has a negligible effect on this broadening. At the same time,

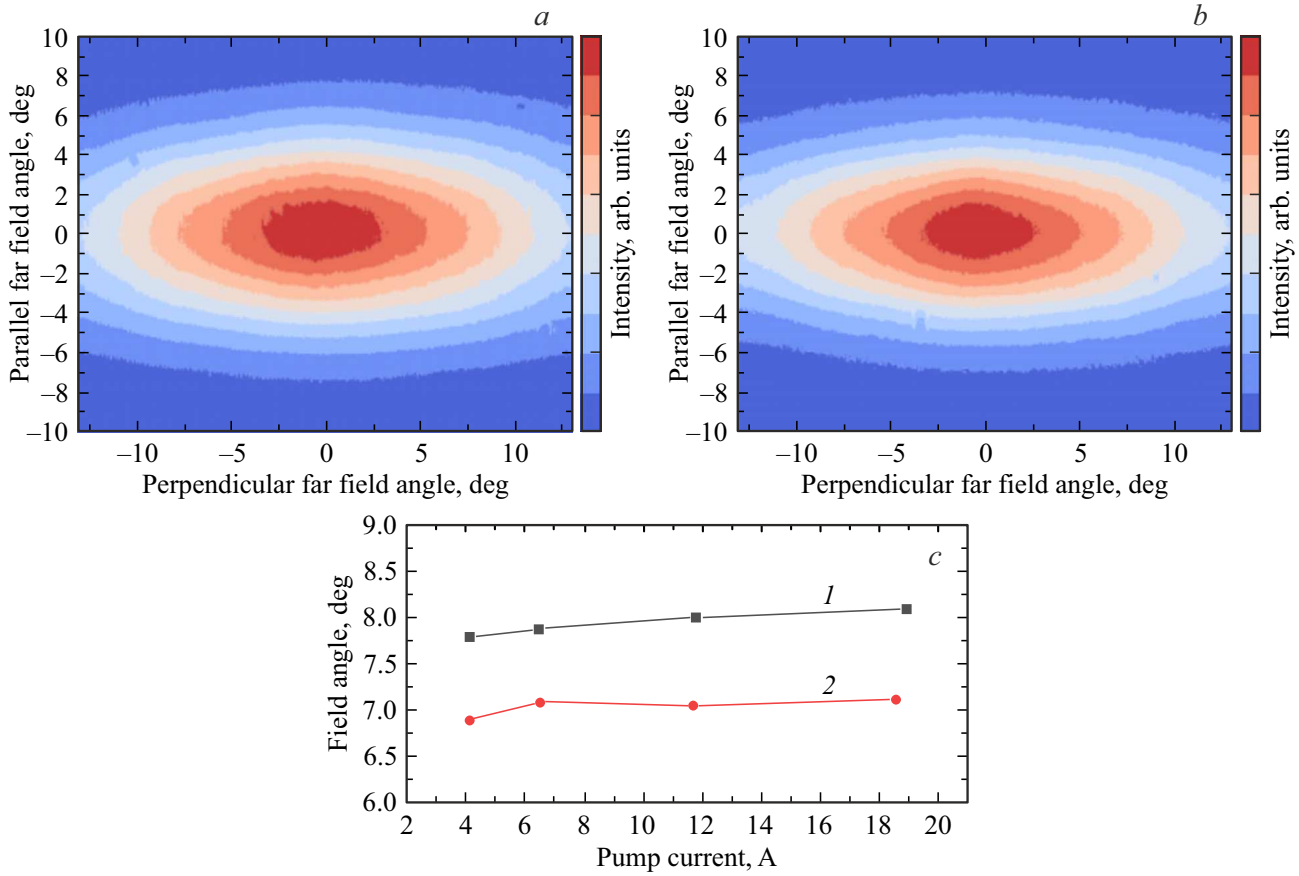

Figure 7. Typical radiation patterns of microstripe bars: *a* — HDMSA and *b* — LDMSA. *c* — FWHM slow-axis divergence for HDMSA and LDMSA microstripe bars at different pump current amplitudes (the shape of pulses corresponds to Figure 2, *a*). (A color version of the figure is provided in the online version of the paper).

microstripe bars demonstrated a stable radiation pattern corresponding to the fundamental optical mode with a high quality of the lateral field and a divergence of 7.9×22.8 (HDMSA design) and $7 \times 24.9°$ (LDMSA design) along two axes. This an important factor for assembly of optical beam-shaping systems for lidars and rangers.

Acknowledgments

The authors would like to thank P.S. Gavrina for her assistance in preparation of the manuscript.

Conflict of interest

The authors declare that they have no conflict of interest.

References

[1] D.F. Zaitsev, V.M. Andreev, I.A. Bilenko, A.A. Berezovskii, P.Yu. Vladislavskii, Yu.B. Gurfinkel', L.I. Tsvetkova, V.S. Kalinovskii, N.M. Kondrat'ev, V.N. Kosolobov, V.F. Kurochkin, S.O. Slipchenko, N.V. Smirnov, B.V. Yakovlev. Radiotekhnika, **85**, 153 (2021). (in Russian). DOI: 10.18127/j00338486-202104-17

[2] N.H. Zhu, Z. Shi, Z.K. Zhang, Y.M. Zhang, C.W. Zou, Z.P. Zhao, Y. Liu, W. Li, M. Li. IEEE J. Select. Topics Quant. Electron., **24**, 1 (2018). DOI: 10.1109/JSTQE.2017.2720959

[3] J.M.T. Huikari, E.A. Avrutin, B.S. Ryvkin, J.J. Nissinen, J.T. Kostamovaara. IEEE J. Select. Topics Quant. Electron., **21**, 1501206 (2015). DOI: 10.1109/JSTQE.2015.2416342

[4] A.A. Podoskin, I.V. Shushkanov, V.V. Shamakhov, A.E. Rizaev, M.I. Kondratov, A.A. Klimov, S.V. Zazulin, S.O. Slipchenko, N.A. Pikhtin. Kvantovaya Elektron., **53**, 1 (2023). (in Russian).

[5] B. Ryvkin, E.A. Avrutin, J.T. Kostamovaara. J. Lightwave Technol., **27**, 2125 (2009). DOI: 10.1109/JLT.2008.2009075

[6] V.S. Golovin, S.O. Slipchenko, A.A. Podoskin, A.E. Kazakova, N.A. Pikhtin. J. Lightwave Technol., **40**, 4321 (2022). DOI: 10.1109/JLT.2022.3159574

[7] E.A. Avrutin, B.S. Ryvkin, J.T. Kostamovaara, D.V. Kuksenkov. Semicond. Sci. Technol., **30**, 055006 (2015). DOI: 10.1088/0268-1242/30/5/055006

[8] S.O. Slipchenko, A.A. Podoskin, V.S. Golovin, N.A. Pikhtin, P.S. Kop'ev. IEEE Photon. Techn. Lett., **33**, 7 (2020). DOI: 10.1109/LPT.2020.3040063

[9] S.O. Slipchenko, I.S. Shashkin, D.A. Veselov, V.A. Kriychkov, A.E. Kazakova, A.Y. Leshko, V.V. Shamakhov, D.N. Nikolaev, N.A. Pikhtin. J. Lightwave Technol., **40**, 2933 (2022). DOI: 10.1109/JLT.2022.3144663

[10] R.J. Lang, A.G. Larsson, J.G. Cody. IEEE J. Quant. Electron., **27**, 312 (1991). DOI: 10.1109/3.81329
[11] G.M. Smith, L.J. Missaggia, M.K. Connors, J.P. Donnelly, R.B. Swint, G.W. Turner, M. Dogan, J.H. Jacob. *2014 Int. Semiconductor Laser Conf.*, Palma de Mallorca, Spain, 2014 (IEEE 2014 Int. Semiconductor Laser Conf.) p. 199. DOI: 10.1109/ISLC.2014.232
[12] L.A. Coldren, S.W. Corzine, M.L. Mashanovitch. *Diode lasers and photonic integratedcircuits* (John Wiley & Sons, 2012). DOI: 10.1002/9781118148167

Translated by D.Safin